Received: 5 May 2018 | Accepted: 2 October 2018

DOI: 10.1002/jcp.27659

ORIGINAL RESEARCH ARTICLE

WILEY Journal of Cellular Physiology

Aβ stimulates microglial activation through antizyme-dependent downregulation of ornithine decarboxylase

Yu-Wen Cheng[1*] | Chun-Cheng Chang[2*] | Ti-Sheng Chang [2] | Hsin-Hua Li[3] | Hui-Chih Hung[4] | Guang-Yaw Liu[5] | Chih-Li Lin[3,6]

[1]Department of Internal Medicine, Yuanli Lee's General Hospital, Lee's Medical Corporation, Miaoli, Taiwan

[2]Department of Internal Medicine, Dajia Lee's General Hospital, Lee's Medical Corporation, Taichung, Taiwan

[3]Institute of Medicine, College of Medicine, Chung Shan Medical University, Taichung, Taiwan

[4]Department of Life Sciences and Institute of Genomics and Bioinformatics, National Chung Hsing University, Taichung, Taiwan

[5]Institute of Biochemistry, Microbiology and Immunology, College of Medicine, Chung Shan Medical University, Taichung, Taiwan

[6]Department of Medical Research, Chung Shan Medical University Hospital, Taichung, Taiwan

Correspondence
Chih-Li Lin, Ph.D./Associate Professor, Institute of Medicine, Chung Shan Medical University, No. 110, Sec. 1, Jianguo N. Rd., Taichung City 402, Taiwan.
Email: dll@csmu.edu.tw

Funding information
National Chung Hsing University and Chung Shan Medical University, Grant/Award Number: NCHU-CSMU-10503; Ministry of Science and Technology, Taiwan, Grant/Award Number: MOST 106-2320-B-040-021-MY3

Abstract

Alzheimer's disease (AD) is one of the most prevalent neurodegenerative disorders. Its pathology is associated with the deposition of amyloid β (Aβ), an abnormal extracellular peptide. Moreover, its pathological progression is closely accompanied by neuroinflammation. Specifically, Aβ-associated microglial overactivation may have the central role in AD pathogenesis. Interestingly, arginine metabolism may contribute to the equilibrium between M1 and M2 microglia. However, little is known about the involvement of arginine metabolism in Aβ-induced microglial neuroinflammation and neurotoxicity. Moreover, the underlying mechanism by which Aβ induces the transition of microglia to the M1 phenotype remains unclear. In this study, we investigated the role of Aβ in mediating microglial activation and polarization both in vitro and in vivo. Our results demonstrated that under the Aβ treatment, ornithine decarboxylase (ODC), a rate-limiting enzyme in the regulation of arginine catabolism, regulates microglial activation by altering the antizyme (AZ) + 1 ribosomal frameshift. Furthermore, the restoration of ODC protein expression levels has profound effects on inhibition of Aβ-induced M1 markers and thus attenuates microglial-mediated cytotoxicity. Altogether, our findings suggested that Aβ may contribute to M1-like activation by disrupting the balance between ODC and AZ in microglia.

KEYWORDS
alzheimer's disease, amyloid β, antizyme, microglia, ornithine decarboxylase

1 | INTRODUCTION

Alzheimer's disease (AD) is a common neurodegenerative disorder that exerts a major impact on the elderly population. The pathology of AD can be attributed to the deposition of an extracellular abnormal protein called amyloid β (Aβ). Aβ deposition in the AD brain is known to cause synaptic loss and neuronal apoptosis. Interestingly, Aβ is not only directly toxic but also stimulates a harmful inflammatory response in neurons. In particular, chronic inflammation caused by microglia may have a major role in AD pathogenesis (Cheng-Chung Wei et al., 2016). Microglial cells are immune cells that localize entirely in the central nervous system. Under normal conditions, microglia exhibit a ramified cell morphology that is generally designated as the resting state. Once activated, their morphology changes to amoeboid, and they become inflammatory. Activated microglia may adopt the M1 or M2 phenotype on the basis of their activation states (Tang & Le, 2016). Generally, M1 microglia have a proinflammatory role in facilitating pathogen destruction. By

*Yu-Wen Cheng and Chun-Cheng Chang contributed equally to this study.

 © 2018 Wiley Periodicals, Inc.

contrast, M2 microglia are implicated in inhibiting inflammation and restoring homeostasis; these functions protect against excessive inflammatory injuries (Pena-Altamira et al., 2017). M1 and M2 microglia maintain a dynamic balance by releasing various cytokines under different conditions (Donat, Scott, Gentleman, & Sastre, 2017). However, Aβ deposition in the brains of patients with AD may provoke chronic and unregulated neuroinflammation, which ultimately results in microglial-mediated neurotoxicity, neuronal dysfunction, and neuronal cell death (Doens & Fernandez, 2014). Aβ-stimulated microglia are predominantly M1 in phenotype, suggesting that Aβ may contribute to M2-to-M1 transition (McGeer & McGeer, 2015). Although microglial-mediated neuroinflammation has been established as an essential cofactor in AD pathogenesis (Clarke, O'Connell, Lyons, & Lynch, 2007; Murphy et al., 2011), the underlying mechanism by which Aβ causes the transition to the M1 microglial phenotype remains unclear.

The arginine metabolism pathway may be involved in the regulation of M1/M2 microglial polarization (Andreasson et al., 2016). Arginine is an amino acid essential for the physiological functions of the central nervous system. Arginine participates in nitric oxide (NO) synthesis through the action of the enzyme NO synthase. NO synthase, particularly the inducible nitric oxide synthase (iNOS), is mainly expressed by M1 microglia (Orihuela, McPherson, & Harry, 2016). In response to a specific trigger, activated M1 microglia can produce a large array of cytotoxic factors, such as NO, superoxide, interleukin-1β (IL-1β), and tumor necrosis factor-α (TNF-α), resulting in inflammation-mediated oxidative stress and neurodegeneration (McPherson, Merrick, & Harry, 2014). Conversely, arginine can also be degraded by the enzyme arginase-1 (Arg1), which is highly expressed in M2 microglia (Cherry, Olschowka, & O'banion, 2014). Arg1 converts arginine to the cationic amino acid ornithine, which can be further catabolized by ornithine decarboxylase (ODC). Interestingly, Arg1 can compete with iNOS for the common substrate arginine, suggesting that metabolic shifts through the upregulation of the arginase metabolic pathway may be involved in inducing or maintaining the M2 polarization of microglia. Although Arg1-expressed microglia are resistant to Aβ-derived neuroinflammation and neurotoxic effects in vivo (Cherry, Olschowka, & O'banion, 2015), the molecular mechanisms that control arginine metabolism remain to be elucidated in further detail.

Given that M1 microglia are strongly implicated in the pathogenesis of AD, the contribution of Aβ to microglial overactivation through the promotion of M2-to-M1 transition should be investigated. In the arginine–arginase metabolic pathway, Arg1 synthesizes ornithine, which is subsequently converted into polyamines by ODC (Colton, 2009). Polyamines, such as putrescine, spermidine, and spermine, are small cationic molecules that participate in various cellular physiological functions (Ramani, De Bandt, & Cynober, 2014). For example, spermidine attenuates production of proinflammatory cytokines by microglia, suggesting that polyamines may be involved in the regulation of microglial activation (Choi & Park, 2012). Moreover, deletion of ODC increases chronic inflammation and macrophage M1 activation (Hardbower et al., 2017). Given that ODC is the key enzyme of polyamine biosynthesis, it is tightly regulated by the protein antizyme (AZ). AZ can bind to ODC and trigger ODC proteolysis, thus markedly reduces ODC and polyamine biosynthesis. In addition, AZ inhibits the cellular uptake of extracellular polyamines, indicating that AZ can negatively regulate polyamine levels. Interestingly, the regulation of AZ messenger RNA (mRNA) frameshifting has a central role in ODC homeostasis. Excess polyamine levels stimulate a + 1 ribosomal frameshift in the translation of AZ mRNA. This frameshift mutation leads to the expression of a full-length and functional protein, consequently upregulating AZ biosynthesis and downregulating ODC and polyamine biosynthesis (Kahana, 2016). Although, ODC is implicated in the chronic microglial activation of AD pathology, the mechanisms, particularly the effects of M1/M2 microglial polarization, that underlie the Aβ-mediated arginase/ODC/polyamine axis remain to be fully defined. Therefore, in the current study, we investigated the role of Aβ in mediating microglial activation and polarization. Our findings suggested that Aβ may contribute to M1-like activation by disrupting the balance between ODC and AZ in microglia.

2 | MATERIALS AND METHODS

2.1 | Materials

Chemicals, such as 3-(4,5-dimethylthiazol-2-yl)-2,5-diphenyltetrazolium bromide (MTT), 4′,6-diamidino-2-phenylindole (DAPI), and nitroblue tetrazolium were purchased from Sigma-Aldrich (München, Germany). All chemicals were prepared through dissolution in phosphate-buffered saline (PBS) solution and stored at −20°C until use. A wild-type ODC-overexpressing plasmid was constructed in our laboratory and proven to be highly effective in our previous study (Huang et al., 2005). Antibodies against p-IκBα, IκBα, p-p65, p65, pERK, ERK, caspase 3, PARP, p-Akt, Akt, ODC, COX-2, Arginase 1, Iba1 (all from Santa Cruz Biotechnology, Santa Cruz, CA), p-p38, p38, p-JNK, JNK, p-IRS-1, IRS-1 (all from Cell Signaling Technology, Beverly, MA), iNOS (from Alexis Biochemicals, San Diego, CA), CD11b (from Abcam, Cambridge, MA), AZ (from Mdbio, Taipei, Taiwan), PE-CD206 (from BD Biosciences, Bedford, MA), and β-actin (from Novus Biologicals, Littleton, CO) were used. Aβ 1–42 was synthesized by LifeTein (Somerset, NJ), and Aβ lyophilized peptides were prepared and resuspended in anhydrous dimethyl sulfoxide (DMSO) as our previously described (Cheng-Chung Wei et al., 2016).

2.2 | Cell culture and viability assay

The BV2 mouse microglial cell line used in this study was kindly gifted by Dr. Yen-Chou Chen from Taipei Medical University, Taiwan. Neuro-2a mouse neuroblastoma cells (BCRC 60026) were purchased from Bioresources Collection and Research Center (BCRC, Hsinchu, Taiwan). Both cell lines were maintained in Dulbecco's modified Eagle's medium (DMEM) supplemented with 10% heat-inactivated fetal bovine serum, 100 units/ml penicillin, 100 μg/ml streptomycin, and 2 mM L-glutamine and incubated at 37°C in a humidified

atmosphere of 5% CO_2. For cell viability tests, cells were seeded in a 24-well plate overnight and then treated under the indicated conditions. After 24 hr, MTT was added to the medium in accordance with the manufacturer's instructions. Only viable cells can metabolize MTT into a purple formazan product, the optical density of which was quantified by a Jasco V-700 spectrophotometer (JASCO, Tokyo, Japan) at 550 nm. The average population number of control cells was set to 100% to enable the comparison of the survival rates of other tested cells.

2.3 | mRNA expression analysis by reverse-transcription quantitative PCR (qPCR)

mRNA levels were quantified as previously described (Cheng-Chung Wei et al., 2016). After the treatment, total mRNA was extracted using a RNeasy Kit (Qiagen, Germantown, MD) and spectrophotometrically quantified. The extracted mRNA was reverse-transcribed to complementary DNA (cDNA) by using a TProfessional Thermocycler (Biometra, Göttingen, Germany) under the following conditions: Primer binding at 25°C for 10 min, reverse transcription at 37°C for 120 min, and reverse-transcriptase denaturation at 85°C. Then, mRNA was quantified through real-time polymerase chain reaction (qRT-PCR) with an ABI 7300 Sequence Detection System (Applied Biosystems, Foster City, CA). Target genes were amplified using Power SYBR Green PCR Master Mix (Applied Biosystems) in accordance with the manufacturer's instructions. Each cDNA sample was tested in triplicate. The following temperature parameters were used: initial denaturation at 95°C for 10 min; 40 cycles of denaturation at 95°C for 15 s; annealing at 60°C for 1 min; and dissociation at 95°C for 15 s, 60°C for 15 s, and 95°C for 15 s. The following primer pairs were used: forward 5′-AGG CAC TCC CCC AAA AGA TG-3′ and reverse 5′-TGA GGG TCT GGG CCA TAG AA-3′ for TNF-α; forward 5′-AGG GCT CTT CGG CAA ATG TA-3′ and reverse 5′-GAA GGA ATG CCC ATT AAC AAC AA-3′ for IL-6; forward 5′-GCC CAT CCT CTG TGA CTC AT-3′ and reverse 5′-AGG CCA CAG GTA TTT TGT CG-3′ for IL-1β; forward 5′-TGC TTC CGG AGC TGT GAT CT-3′ and reverse 5′- CGG ACA GAG CGA GCT GAC TT-3′ for IGF-1; forward 5′-AGA CCA CAG TCT GGC AGT TG-3′ and reverse 5′-CCA CCC AAA TGA CAC ATA GG-3′ for arginase 1; forward 5′-TGG CAT GTC CTG GAA TGA T-3′ and reverse 5′-CAG GTG TGG GCT CAG GTA GT-3′ for CD206; and forward 5′-TGG TAT CGT GGA AGG ACT CAT GAC-3′ and reverse 5′-ATG CCA GTG AGC TTC CCG TTC AGC-3′ for GAPDH. Relative mRNA expression values were obtained by using an SDS version 1.2.3 (Sequence Detection Systems 1.2.3-7300 Real-Time PCR System; Applied Biosystems). These values were standardized by comparison with those of the relative expression of GAPDH. All data are obtained from three independent experiments.

2.4 | Western blot analysis

Cells were harvested and homogenized with protein extraction lysis buffer containing 50 mM Tris-HCl at pH 8.0, 5 mM ethylenediaminetetraacetic acid, 150 mM sodium chloride, 0.5% Nonidet P-40, 0.5 mM dithiothreitol, 1 mM phenylmethylsulfonyl fluoride, 0.15 units/ml aprotinin, 5 μg/ml leupeptin, 1 μg/ml pepstatin, and 1 mM sodium fluoride. The solution was centrifuged at 12,000 × *g* for 30 min at 4°C to remove debris, and the supernatant cell lysate was used for immunoblotting analysis. Equal amounts (50 μg) of total proteins from the cell lysate were resolved through sodium dodecyl sulfate-polyacrylamide gel electrophoresis (SDS-PAGE), transferred onto polyvinylidene difluoride membranes (Millipore, Bedford, MA), and then probed with a primary antibody followed by another secondary antibody conjugated with horseradish peroxidase. Primary antibodies were used at a dilution of 1:1,000 in 0.1% Tween-20, and secondary antibodies were used at a dilution of 1:5,000. Immunocomplexes were visualized using enhanced chemiluminescence kits (Millipore). The relative expression levels of proteins were densitometrically quantified using ImagePro Plus 6.0 software (Media Cybernetics, Silver Spring, MD), further normalized on the basis of the expression level of the housekeeping protein β-actin, and then compared with the normalized protein levels of control cells. The control protein level was then set to 100% for further comparison. All data are obtained from three independent experiments.

2.5 | Polyamines determination by high-performance liquid chromatography (HPLC)

Cells were harvested, transferred to centrifuge tubes, and washed twice with ice-cold PBS. Then, 200 μl of ice-cold 1.5 M HClO4 was added to the cells. The cells were then vortexed for 1 min at room temperature. After vortexing, 100 μl of ice-cold 2 M K_2CO_3 was added to the mixture. The centrifuge tube was left uncapped for 1 min to allow the evaporation of CO_2. The tubes were then recapped, vortexed for 1 min at 25°C, uncapped to release extra gas, and then recapped. The mixture was centrifuged at 15,000 ×*g* at 4°C for 10 min. The supernatant was collected for high-performance liquid chromatography (HPLC) analysis. The polyamines putrescine, spermidine, and spermine were separated using an HPLC system (JASCO Model PU- 2080, Tokyo, Japan). Gradient-mode chromatography was performed using a separate reverse-phase HPLC (RP-HPLC) system, as follows: Fractionation was performed with a LUNA C18 analytical column packed with 5 μm particles (250 mm × 4.6 mm; Phenomenex, Torrance, CA) and equipped with a guard column. The scouting gradient was a linear gradient from the 70% mobile phase A (0.1 M sodium acetate pH 7.2) to 100% mobile phase B (100% HPLC-grade methanol) at a flow rate of 1.0 ml/min over approximately 20 min. The signal was monitored at an excitation wavelength of 340 nm and an emission wavelength of 450 nm (FP-2020 Plus Intelligent Fluorescence Detector; Jasco). SISC-32 data process software (SISC, Taipei, Taiwan) was used to record and analyze HPLC data.

2.6 | Cell transfection, ODC overexpression, and AZ + 1 frameshift activity assay

For ODC overexpression, BV2 cells were transfected with ODC or empty plasmid. Human full-length human ODC1 was obtained from

Addgene (Cambridge, MA) and cloned in pcDNA3.1 expression vector. For AZ frameshift activity assay, cells were transfected with a dual-luciferase reporter assay system plasmid (Promega Life Sciences, Madison, WI) containing partially overlapping open reading frame 1 (ORF1) and open reading frame 2 (ORF2) sequences of AZ. ORF1 encodes for a 68 amino acids nonfunctional peptide in length and is terminated by a UGA stop codon. Moreover, this plasmid constitutively expresses *Renilla* luciferase. Once the +1 frameshifting of AZ occurs, the UGA stop codon of AZ ORF1 changes to a sense codon, which results in the translation of ORF2 and the synthesis of the second firefly luciferase. The dual-luciferase assay is performed by sequentially measuring the firefly and *Renilla* luciferase activities of the same sample, with the results expressed as the ratio of firefly to *Renilla* luciferase activity represented as +1 frameshift efficiencies of AZ. For transfection, cells were cultured in 6-well plate, and 2 μg plasmid were transfected after 24 hr with 5 μl Lipofectamine 2000 (Life Technologies). Transfections and media changes were performed according to the manufacturers' optimized protocols. After 24 hr of transfection, cells were then treated under the indicated conditions. Thereafter, cell lysates were prepared using reporter lysis buffer (Promega Life Sciences), and luciferase activity was measured immediately using a SpectraMax M5 Multi-Mode Microplate Reader (Molecular Devices, Sunnyvale, CA). Firefly luciferase luminescence was read at a wavelength of 560 nm, and *Renilla* luciferase luminescence was read at a wavelength of 480 nm. All data are obtained from five independent experiments.

2.7 | Flow cytometry analysis of CD206 in BV2 cells

At the end of the experiments, cells were harvested and analyzed for the presence of cell-surface antigens through staining with PE-CD206 antibody. The cells were gated using forward and sideward scatter characteristics, and at least 10,000 gated events were collected using a NovoCyte flow cytometer (NovoCyte 2000, ACEA Biosciences, San Diego, CA). Data were analyzed using a NovoExpress analysis software (ACEA Biosciences). All data are obtained from three independent experiments.

2.8 | Treatment of Neuro-2a cells with BV2-conditioned medium

BV2 microglia were stimulated in the presence or absence of 5 μM Aβ under the indicated conditions for 24 hr and then centrifuged to obtain a cell-free supernatant. Neuro-2a neuronal cells were serum-starved for 4 hr and treated with 50% BV2-conditioned medium and 50% fresh DMEM. After 24 hr of incubation, the viability of Neuro-2a cells was determined through MTT and superoxide radical anion determination assays. Levels of intracellular superoxide radical anions were quantified through staining with dihydroethidium (DHE), a fluorogenic reagent. Superoxide radical levels were quantified following previously reported procedures (Li et al., 2016). Briefly, cells were treated in fresh medium containing 10 μM DHE and incubated for 30 min in the dark at room temperature. After 30 min of incubation, the staining medium was discarded. Cells were washed twice with PBS and then observed and photographed under an inverted fluorescence microscope (DP72/CKX41, Olympus, Tokyo, Japan). All data are obtained from three independent experiments.

2.9 | Stereotaxic intracerebroventricular injection of Aβ in rats

Twelve-week-old Sprague Dawley (SD) rats were kept on a 12 hr light/dark cycle and housed individually with free access to food and water. The rats were randomly divided into two groups with six rats per group (sham and Aβ). All animal experiments were approved by the animal experimental committees of Chung Shan Medical University, Taiwan (CSMU No. 1689) and performed in accordance with the guidelines and regulations of the Institutional Animal Care and Use Committee. The intracerebral injection protocol was performed in reference to previous studies (Lin et al., 2016). Briefly, 5 μl of $A\beta_{1-42}$ solution (2 μg/μl, 10 μg each side) or saline was injected into each side of the hippocampus CA1 by using the following stereotaxic coordinates: 2.8 mm posterior to the bregma, 2.6 mm left/right to the midline, and 3.0 mm ventral to the bregma. After stereotaxic injection, rats were singly housed to assure optimal recovery from surgery. After 6 weeks of intracerebral injection, the animals were killed, and brains were collected by using a freezing microtome (CM 3050S Cryostat, Leica, Germany). Hippocampal slices were analyzed through immunohistochemistry or fluorescence microscopy.

2.10 | T-maze assessments

Working memory was assessed using the T-maze test. The rats learned to find food rewards in the T-maze using their working memory, and the percentage of correct responses and time latency were recorded. At 4 weeks after intracerebral injection, the rats were subjected to behavioral tests, which were performed as previously described (Hsieh et al., 2017). Each rat underwent two training sessions (on days 1 and 2) and one test session (on Day 3). Each training session consisted of nine trials. Data were collected and analyzed by the SMART video tracking system (SMART v3.0, Panlab SL, Barcelona, Spain).

2.11 | Immunocytochemistry and immunofluorescence staining

After 1 week of behavioral testing, rats were euthanized through deep anesthetization with isoflurane and then perfused with ice-cold PBS followed by chilled 4% paraformaldehyde in PBS. Brains were fixed and maintained in 30% sucrose solution and stored at 4°C until ready for cryostat sectioning. For immunohistochemistry staining, coronal sections of the hippocampal tissues were blocked

by incubation for 1 hr at room temperature in 10% normal goat serum (Sigma-Aldrich) containing 0.5% Triton X-100 (Sigma-Aldrich). The slides were then incubated overnight at 4°C with antiIba1. The slides were then incubated sequentially: first, with biotinylated horse antiIgG antibodies for 1 hr at room temperature; then with streptavidin–horseradish peroxidase for 30 min at 37°C; and finally with 3,3′-diaminobenzidine tetrachloride 10 min at room temperature (Sigma-Aldrich). For immunofluorescence staining, the slides were fixed with 2% buffered paraformaldehyde, permeabilized in 0.25% Triton X-100 for 5 min at 4°C, and then incubated with antiIba1 or anti-ODC. The slides were then incubated with a FITC- or Rhodamine-labeled second antibody (Santa Cruz) depending on the origin of the primary antibody. All slides were viewed using a fluorescence microscope (DP80/BX53; Olympus) and cellSens version 1.9 digital imaging software.

2.12 | Statistical analysis

All data are presented as means ± standard error of the mean. The statistical significance of differences between compared groups was determined through one-way analysis of variance following Dunnett's post hoc test for multiple comparisons with SPSS Statistics version 22.0 software (SPSS Inc., Chicago, IL). A probability value of < 0.05 or < 0.01 was specified to indicate statistical significance.

3 | RESULTS

3.1 | Aβ induces BV2 microglial activation and mediates proinflammatory responses

Exogenous Aβ induces microglial activation and increases proinflammatory cytokine secretion. In this study, we used the immortalized murine microglial cell line BV2 to establish an in vitro model of Aβ-mediated microglial activation. Transcriptome and proteome analyses have shown that BV2 cells display a high similarity with primary microglial cells, suggesting their suitable applications in studies on cellular and molecular changes in neuroinflammatory response (Henn et al., 2009). To investigate the cellular compatibility of Aβ with BV2 microglia, we determined the viabilities of BV2 microglia treated with 2.5 μM–10 μM of $A\beta_{1-42}$ for 24 hr through the MTT assay. Figure 1a shows that treatment with less than 5 μM of Aβ exerted no significant cytotoxic effects. Therefore, we used this concentration of Aβ in our subsequent experiments. In addition, we observed morphological changes under an inverted microscope. It is known that BV2 cells can transform from a ramified basal homeostatic phenotype to an activated phagocytic phenotype in response to neurodegenerative stress (Dang et al., 2014). As shown in Figure 1b, the basal homeostatic microglia have a ramified shape (blue arrows). Conversely, Aβ-treated BV2 cells convert to round and amoeboid

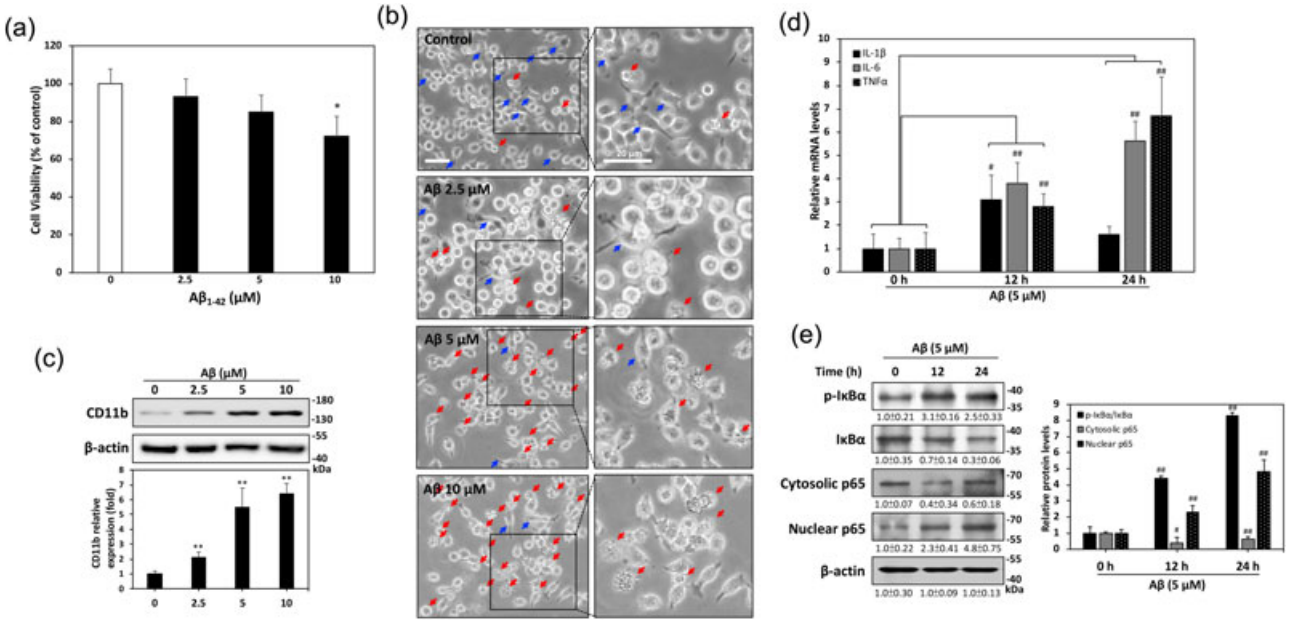

FIGURE 1 Aβ stimulates microglial activation and inflammatory responses in BV2 microglia. (a) Effects of Aβ on the viability of BV2 microglia. Cells were treated with the indicated concentrations of Aβ for 24 hr, and cell survival was evaluated through MTT assay. (b) Representative images of BV2 microglia incubated with Aβ for 24 hr. Red arrows indicate the activated BV2 cells. Blue arrows indicate the basal homeostatic BV2 cells. (c) CD11b protein expression was measured by western blot analysis. 24 hr Aβ treatment significantly increased the levels of CD11b in BV2 cells. (d) mRNA expression levels of IL-1β, IL-6, and TNF-α proinflammatory cytokines were measured through real-time qPCR and normalized to that of the reference gene *GAPDH*. (e) Protein expression levels of p-IκB-α, IκB-α, cytosolic p65, and nuclear p65 were determined through western blot analysis with specific antibodies. All data were obtained from three independent experiments, and values were expressed as mean ± SEM. $^{*}p < 0.05$ and $^{**}p < 0.01$ of experimental groups were compared with those of control groups, and $^{\#}p < 0.05$ and $^{\#\#}p < 0.01$ were compared with the 0 hr group for multiple comparisons through Dunnett's post hoc test. Scale bar represents 20 μm. mRNA: messenger RNA; MTT: 3-(4,5-dimethylthiazol-2-yl)-2, 5-diphenyltetrazolium bromide; qPCR: quantitative polymerase chain reaction [Color figure can be viewed at wileyonlinelibrary.com]

shapes within 24 hr (red arrows). These morphological changes suggest that Aβ stimulation may promote BV2 cells to adopt an amoeboid shape. To further confirm these findings, we analyzed the expression of CD11b, an indicator of microglial activation (Roy et al., 2008). As shown in Figure 1c, 24 hr of Aβ treatment increased the levels of CD11b protein expression, indicating that BV2 cells are indeed activated by Aβ stimuli. To investigate the inflammatory effects of Aβ on microglial activation, we performed qPCR analysis to quantify the mRNA levels of some proinflammatory cytokines, such as IL-1β, IL-6, and TNF-α. As shown in Figure 1d, 12 hr of treatment with 5 μM Aβ significantly upregulated IL-1β mRNA levels, and 24 hr of treatment markedly elevated IL-6 and TNF-α mRNA levels. Western blot analysis also revealed that the levels of phospho-IκBα and nuclear p65 were also upregulated by Aβ, implying that the activation of the NF-κB pathway is responsible for Aβ-induced microglial inflammation (Figure 1e). Collectively, these results suggested that Aβ stimulation can induce microglial activation.

3.2 | Aβ promotes M1-like polarization and reduces cellular polyamine levels in BV2 microglia

M1 microglia are characterized by the upregulated expression of some proinflammatory mediators, such as iNOS and cyclooxygenase-2 (COX-2). We performed western blot analysis for iNOS and COX-2 to validate whether Aβ can polarize BV2 microglia into M1 phenotype. The results are shown in Figure 2a, indicated that Aβ markedly increased the protein expression levels of iNOS and COX-2, suggesting that M1 polarization is involved in Aβ-stimulated microglial activation. In addition, the Aβ treatment upregulated the phosphorylation of three major mitogen-activated protein kinase (MAPK) subgroups, including JNK, ERK, and p38. These observations are in line with the results of previous studies showing that the MAPK signaling pathway may have a vital role in microglial activation and may be associated with the M2-to-M1 transition process (Bhatia, Baron, Hagl, Eckert, & Fiebich, 2016; Orihuela et al., 2016). To confirm this finding, we identified some M2 microglial markers through qPCR assays. As shown in Figure 2b, Aβ treatment

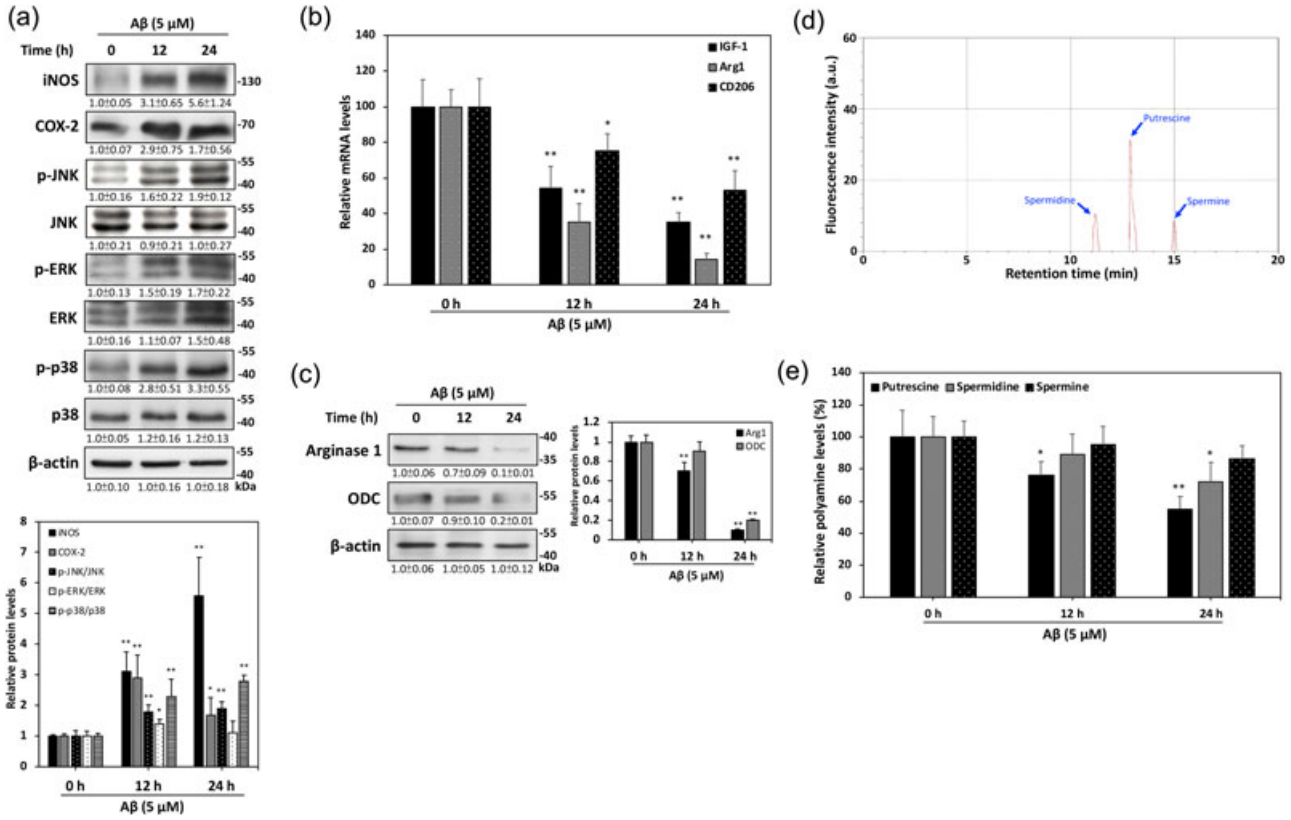

FIGURE 2 Aβ promotes M1-like polarization and reduces polyamine levels in BV2 microglia. (a) Aβ upregulated the expression of proinflammatory M1 markers in BV2 microglia. BV2 cells were treated with 5 μM Aβ for 24 hr, and the protein expression levels of iNOS, COX-2, JNK and phosphorylated JNK, ERK and phosphorylated ERK, and p38 and phosphorylated p38 were determined through western blot analysis with specific antibodies. (b) mRNA levels of M2 markers, including IGF-1, Arg1, and CD206, were measured through qPCR. (c) Protein expression levels of Arg1 and ODC were determined through western blot analysis. (d) Standard HPLC chromatograph of three major polyamine standards, including spermidine, putrescine, and spermine. (e) Quantitative analysis through HPLC revealed that Aβ treatment decreased polyamine levels in BV2 microglia. All data were obtained from three independent experiments, and values were expressed as mean ± SEM. $^{*}p < 0.05$ and $^{**}p < 0.01$ of experimental groups were compared with those of the 0 hr groups for multiple comparisons through Dunnett's post hoc test. HPLC: high-performance liquid chromatography; mRNA: messenger RNA; ODC: ornithine decarboxylase; qPCR: quantitative polymerase chain reaction [Color figure can be viewed at wileyonlinelibrary.com]

significantly suppressed the mRNA levels of three M2 markers, including insulin-like growth factor-1 (IGF-1), Arg1, and CD206, in a time-dependent manner, implying that Aβ has a critical role in M1 polarization. In particular, the mRNA levels of Arg1, a classic M2 marker, decreased in BV2 cells that had been exposed to Aβ for 24 hr. To further verify this result, we performed western blot analysis to detect the levels of Arg1 protein expression in cell extracts. As expected, Aβ treatment not only significantly suppressed the expression of Arg1 at the protein level but also downregulated that of the downstream metabolic enzyme ODC (Figure 2c). This result suggested that Aβ may inhibit polyamine biosynthesis. To determine whether Aβ treatment governs the intracellular level of polyamines in BV2 cells, we measured the levels of the essential polyamines spermidine, putrescine, and spermine through RP-HPLC with the fluorescence detection method (Figure 2d). As shown in Figure 2e, Aβ treatment decreased putrescine and spermidine levels in a time-dependent manner. These findings suggested that Aβ may promote the polarization of BV2 microglia toward an M1-like phenotype. Altogether, this effect parallels the inhibition of polyamine biosynthesis by the downregulation of Arg1 and ODC protein levels.

3.3 | Aβ suppresses ODC protein expression by stimulating the +1 ribosomal frameshift of AZ mRNA in BV2 microglia

Our previous results have demonstrated that the reduction in polyamine levels may be associated with Aβ-induced inhibition of ODC protein expression. AZ plays the most important role in stimulating the posttranslational degradation of ODC. To evaluate whether AZ plays a role in the suppression of ODC by Aβ, we performed western blot analysis to detect the protein expression levels of AZ and ODC in BV2 cells incubated with 5 μM of Aβ for the indicated periods. As shown in Figure 3a, Aβ treatment significantly increased AZ protein levels in a time-dependent manner. Conversely, Aβ gradually decreased ODC protein expression, and the levels of ODC protein expression partially returned to the baseline after 12 hr of treatment. However, 24 hr of Aβ treatment markedly reduced ODC levels, showing that the inhibition of intracellular polyamine levels might be attributed to the induction of AZ-mediated ODC downregulation caused by Aβ. To confirm the role of Aβ in AZ induction, we constructed a dual-luciferase reporter plasmid containing two partially overlapping

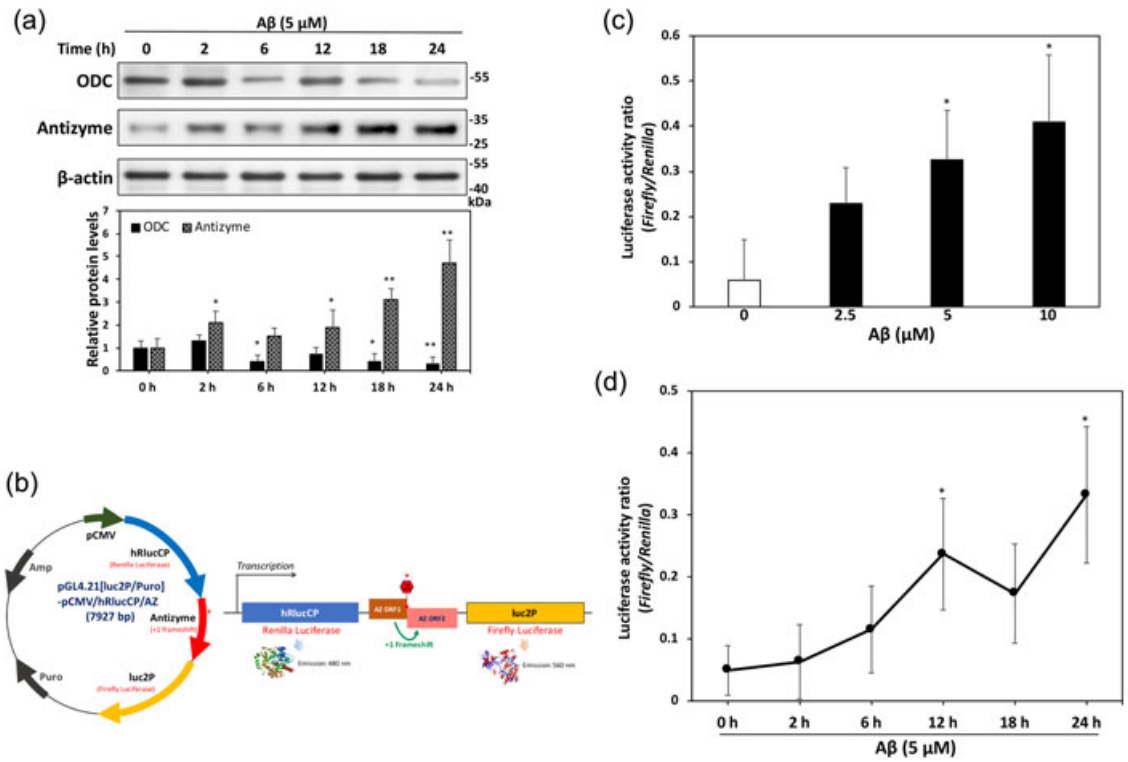

FIGURE 3 Aβ simulates AZ mRNA + 1 ribosomal frameshift and reduces ODC expression in BV2 microglia. (a) Time-dependent western blot analysis of ODC and AZ in BV2 cells incubated with 5 μM Aβ. ODC and AZ expression levels in BV2 cells are inversely related. (b) Scheme of the dual-luciferase reporter plasmid used to measure the + 1 ribosomal frameshifting activity of AZ mRNA. BV2 microglia were treated with the indicated concentrations of Aβ for 24 hr, and AZ mRNA + 1 activities were measured. Data are represented as the ratio of firefly to *Renilla* fluorescence signals. Data indicated that Aβ treatment caused a significant (c) dose- and (d) time-dependent increase in AZ mRNA + 1 frameshifting in BV2 microglia. Western blot data are obtained from three independent experiments, and dual-luciferase reporter data are obtained from five independent experiments. All values are expressed as mean ± SEM. $^{*}p < 0.05$ and $^{**}p < 0.01$ of experimental groups were compared with those of control groups for multiple comparisons through Dunnett's post hoc test. AZ: antizyme; mRNA: messenger RNA; ODC: ornithine decarboxylase [Color figure can be viewed at wileyonlinelibrary.com]

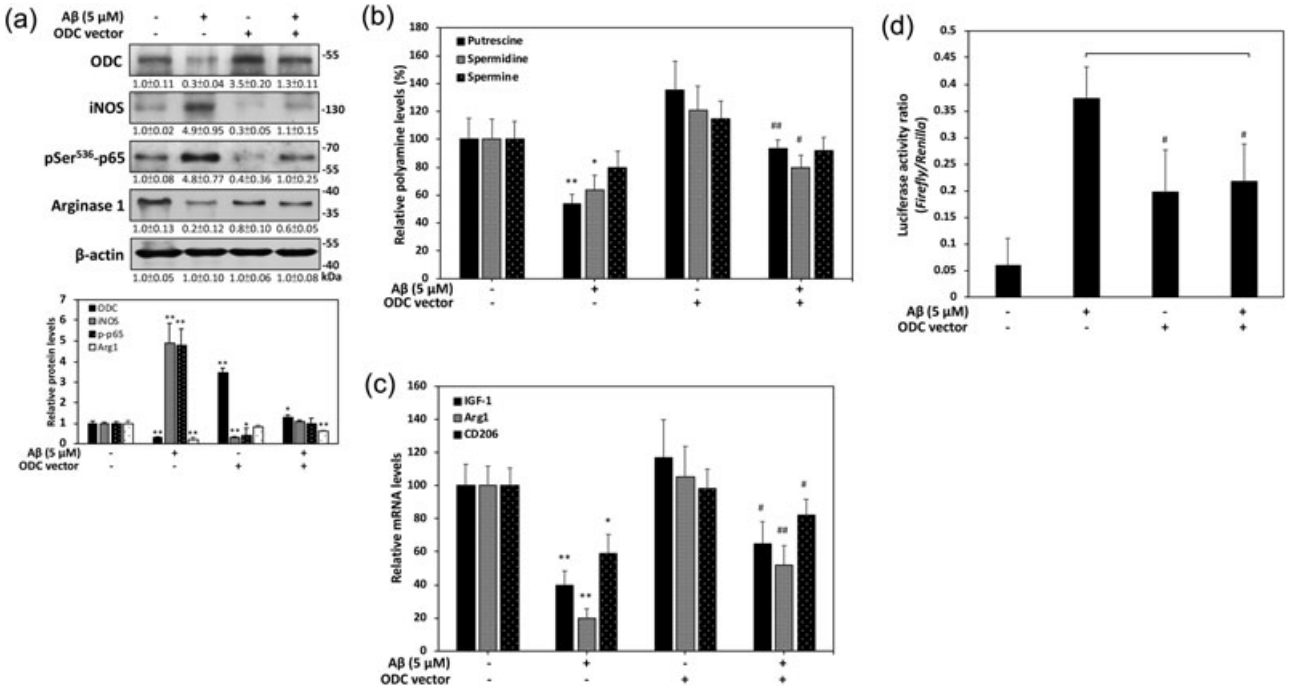

FIGURE 4 ODC overexpression restores intracellular polyamine levels and attenuates Aβ-induced M2-to-M1 phenotypic change in BV2 microglia. (a) Protein expression levels of ODC, iNOS, Ser^{536} phosphorylated p65, and Arg1 were determined through western blot analysis with specific antibodies. (b) Intracellular polyamine levels were measured through HPLC. Results showed that ODC overexpression markedly restored Aβ-induced suppression of putrescine and spermidine intracellular levels. (c) mRNA levels of three microglial M2 markers, including IGF-1, Arg1, and CD206, were measured through qPCR. (d) AZ mRNA + 1 frameshifting activities were measured using the dual-luciferase reporter assay. All data were obtained from three independent experiments, and values were expressed as mean ± SEM. $^{*}p < 0.05$ and $^{**}p < 0.01$ compared with untreated groups, and $^{\#}p < 0.05$ and $^{\#\#}p < 0.01$ were compared with Aβ-treated groups for multiple comparisons by using Dunnett's post hoc test. AZ: antizyme; HPLC: high-performance liquid chromatography; mRNA: messenger RNA; ODC: ornithine decarboxylase; qPCR: quantitative polymerase chain reaction

AZ ORF sequences (Figure 3b). Once Aβ induces the AZ mRNA +1 frameshift, the frameshifting activity will increase in direct proportion to the ratio of firefly to *Renilla* luciferase fluorescence signals. As shown in Figure 3c,d treatment with Aβ for 24 hr caused a dose- and time-dependent increase in the ratio of firefly to *Renilla* fluorescence intensity in BV2 cells. Moreover, stimulation with 5 μM Aβ increased frameshifting intensity by approximately 6-fold relative to that with the control treatment, indicating that AZ levels increase in BV2 microglia via an Aβ-triggered frameshifting mechanism.

3.4 | ODC overexpression reverses Aβ-induced polyamine reduction and M1 markers expression in BV2 microglia

The above results indicated that Aβ induces AZ-mediated polyamine reduction and may suppress the expression of M2-specific markers, suggesting that Aβ-induced microglial M1 polarization may be attenuated by restoring the protein expression levels of ODC. To test this hypothesis, we transiently transfected an ODC overexpression vector into BV2 cells, which were then incubated with 5 μM of Aβ for 24 hr. Immunoblotting results demonstrated that the neuroinflammatory markers iNOS and Ser^{536} phosphorylated NF-κB subunit p65 were significantly elicited by Aβ treatment. However, ODC overexpression effectively inhibited iNOS and NF-κB p65 activation. Similarly, ODC overexpression reversed the Aβ-induced inhibition of the M2 marker Arg1, indicating that the M1/M2 equilibrium of BV2 microglia may be altered by ODC protein levels (Figure 4a). To further determine whether ODC overexpression can effectively compete with Aβ-induced AZ to restore polyamine levels, we examined the influence of ODC overexpression on intracellular polyamine levels. As shown in Figure 4b, ODC overexpression significantly reversed the suppressive effects of Aβ on putrescine and spermidine levels. In addition, ODC overexpression also upregulated the mRNA levels of three major microglial M2 markers, including IGF-1, Arg1, and CD206, relative to that in the Aβ-treated group, suggesting that restoring ODC expression may inhibit microglial polarization from to M1 phenotype (Figure 4c). Accordingly, we observed that ODC overexpression attenuated Aβ-induced AZ mRNA +1 frameshifting (Figure 4d). Taken together, our findings suggested that ODC may protect against Aβ-induced M1 markers expression and polyamine reduction in BV2 microglia.

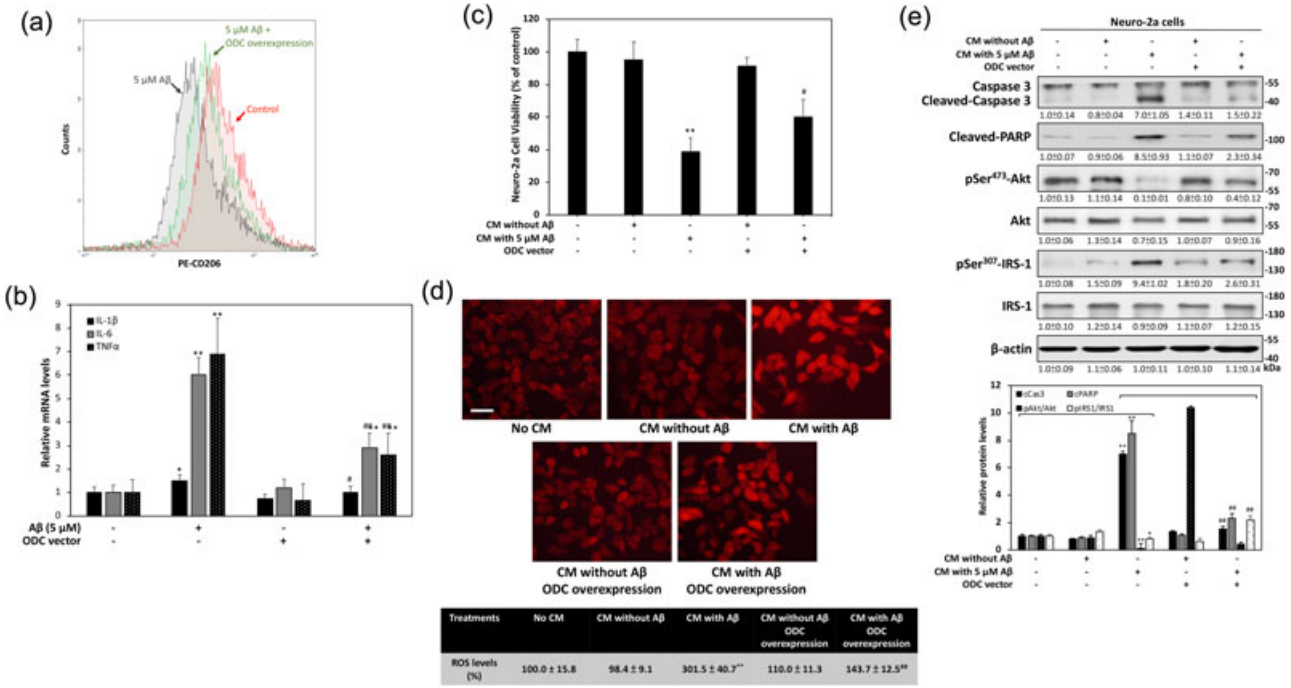

FIGURE 5 ODC overexpression can attenuate Aβ-induced microglial-mediated cytotoxicity in BV2 cells. (a) Flow cytometry histograms showing the staining fluorescence intensity of PE-conjugated CD206 and demonstrating that ODC overexpression restores Aβ-induced inhibition of CD206 membrane expression in BV2 cells. (b) mRNA levels of IL-6, IL-1β, and TNF-α proinflammatory cytokines were measured through qPCR analysis. (c) BV2 microglia were stimulated with 5 μM Aβ in the presence or absence of transient ODC overexpression for 24 hr. Next, Neuro-2a cells were incubated in conditioned media (CM) for 24 hr, and their viabilities were assessed through MTT assays. (d) Intracellular superoxide radical anions stained with dihydroethidium in Neuro-2a cells treated with CM collected from BV2 cells were detected through fluorescence microscopy. Red fluorescence intensities were analyzed and quantified by using Image-Pro Plus 6.0 software. (e) Protein expression levels of caspase 3, cleaved-PARP, p-Akt, Akt, p-IRS-1, and IRS-1 were determined through western blot analysis with specific antibodies. All data are obtained from three independent experiments, and values were expressed as mean ± SEM. $^{*}p < 0.05$ and $^{**}p < 0.01$ compared with untreated groups, and $^{\#}p < 0.05$ and $^{\#\#}p < 0.01$ were compared with Aβ-treated groups for multiple comparisons by using Dunnett's post hoc test. Scale bar represents 20 μm. MTT: 3-(4,5-dimethylthiazol-2-yl)-2, 5-diphenyltetrazolium bromide; mRNA: messenger RNA; ODC: ornithine decarboxylase; qPCR: quantitative polymerase chain reaction [Color figure can be viewed at wileyonlinelibrary.com]

3.5 | Restored ODC expression protects Neuro-2a neuronal cells against Aβ-induced microglial-mediated cytotoxicity

To confirm the role of ODC in the prevention of Aβ-induced M1 polarization, we used flow cytometry to examine the expression of CD206, a well-known M2 surface marker in BV2 microglia. As shown in Figure 5a, the flow cytometry histograms of cells treated with 5 μM Aβ for 24 hr exhibited a peak left-shift of 25% relative to that of the control group, indicating that Aβ markedly reduced CD206 membrane expression in BV2 cells. However, ODC overexpression moderately shifted the curve back, indicating that ODC may help microglial cells shift toward the anti-inflammatory M2-like phenotype. To confirm this hypothesis, we investigated the effect of ODC overexpression on the mRNA levels of M1-related proinflammatory cytokines, including IL-1β, IL-6, and TNF-α, in BV2 cells. Figure 5b sowed that ODC overexpression significantly inhibited the Aβ-induced mRNA expression levels of IL-1β, IL-6, and TNF-α proinflammatory cytokines, suggesting that restoring ODC protein expression may attenuate microglial inflammatory responses and neurotoxicity. Recent evidence has indicated that Aβ may increase neuroinflammation and neurotoxicity through reactive oxygen species-dependent microglial activation (Liu et al., 2017). Therefore, we investigated whether ODC protects against microglial-induced neurotoxicity. We collected conditioned media from BV2 cells that had been stimulated with Aβ for 24 hr. We then treated Neuro-2a cells with the conditioned medium for 24 hr and performed MTT assays to assess cell viability. As shown in Figure 5c, the viability of Neuro-2a cells treated with conditioned media from Aβ-stimulated BV2 cells significantly decreased. By contrast, the viability of Neuro-2a cells treated with conditioned media from ODC-overexpressed BV2 microglia incubated with Aβ markedly increased. These findings were corroborated by the results of dihydroethidium staining for oxidative stress measurement. Specifically, conditioned media from Aβ-stimulated BV2 cells but not from ODC-overexpressed cells significantly increased the levels of intracellular superoxide radical anions in Neuro-2a cells (Figure 5d). This confirmed our hypothesis that the restoration of ODC expression in microglia may attenuate Aβ-induced microglial inflammatory responses and neurotoxicity. Interestingly, recent studies have shown that impaired brain insulin

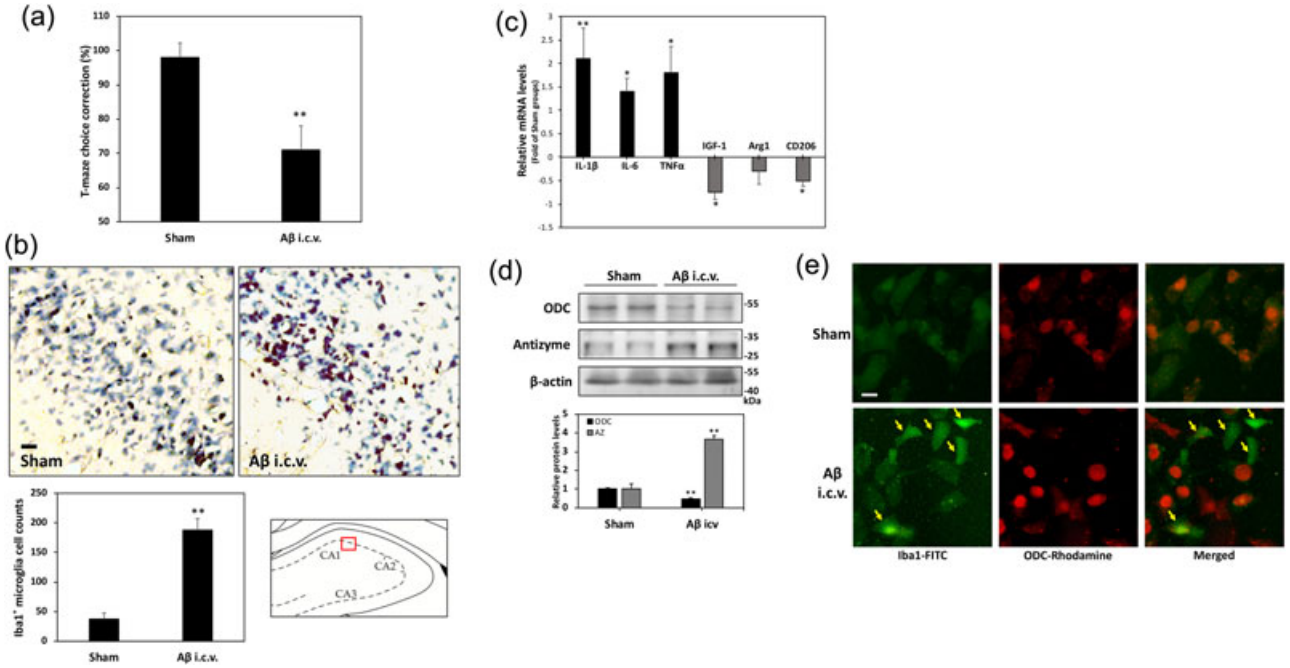

FIGURE 6 Aβ stimulates microglial activation and suppresses ODC protein expression in intra-hippocampal Aβ-injected rats. (a) Behavioral testing was initiated 4 weeks after stereotaxical surgery. Results show the percentage of correct responses for the T-maze test. (b) Iba1$^+$ cells were observed in the hippocampal CA1 region in response to Aβ stimulation. Scale bar represents 20 μm. The number of Iba1$^+$ cells (dark blue) in Aβ-injected rats is significantly higher than those in the sham group. The number of Iba1$^+$ cells was calculated by sampling in five random 400 × fields. (c) mRNA levels of proinflammatory cytokines (IL-1β, IL-6, and TNF-α) and M2 microglial markers (IGF-1, Arg1, and CD206) were elevated through qPCR. (d) Western blot analysis of ODC and AZ hippocampal expression. (e) Immunofluorescence staining of Iba1 (green) and ODC (red) in rat hippocampal slices. The results indicated that ODC protein expression has significantly decreased in the majority of Iba1$^+$ cells (yellow arrows). Scale bar represents 5 μm. Data were expressed as mean ± SEM. $p < 0.05$ and $^{**}p < 0.01$ of experimental groups were compared with those of control groups for multiple comparisons through Dunnett's post hoc test. AZ: antizyme; mRNA: messenger RNA; ODC: ornithine decarboxylase; qPCR: quantitative polymerase chain reaction [Color figure can be viewed at wileyonlinelibrary.com]

signaling is linked to Aβ-related microglial overactivation, suggesting that neuronal insulin resistance may play a role in microglial-induced neurotoxicity (Gad, Zaitone, & Moustafa, 2016). Consistent with previous results, our results demonstrated that conditioned media from Aβ-stimulated BV2 cells significantly increased IRS-1 phosphorylation in Ser^{307}, a typical marker of insulin resistance. However, treating Neuro-2a cells with conditioned media from ODC-overexpressed BV2 cells attenuated the serine phosphorylation of IRS-1 and restored Akt phosphorylation on Ser^{473}. ODC-mediated neuroprotection was also confirmed by inhibiting caspase 3 and PARP cleavage in Neuro-2a cells, as shown in Figure 5e. Taken together, these findings support the idea that the restoration of ODC expression may attenuate the Aβ-induced neurotoxic properties of microglia and contribute to insulin signaling-mediated neuroprotection in neuronal cells.

3.6 | Microglial ODC protein expression is suppressed by the intracerebroventricular injection of Aβ in Wistar rats

Finally, to investigate the in vivo effects of Aβ-mediated ODC expression in microglia, we conducted an animal study based on the stereotaxical bilateral injection of $A\beta_{1-42}$ peptides into the hippocampal CA1 regions of 12-week-old Wistar rats. Working and recognition memory was tested through the T-maze test 4 weeks after surgery. As shown in Figure 6a, the Aβ-injected group showed a significantly lower percentage of correct responses than the sham-operated control group, indicating that Aβ impairs spatial learning. Next, we evaluated whether Aβ induces microglial activation in the brain. Immunohistochemical staining images showed that most Iba1$^+$ cells localized in hippocampal CA1 regions 6 weeks after the intracerebral injection of Aβ (Figure 6b). In addition, the number of Iba1$^+$ cells in the hippocampal CA1 regions of Aβ-injected rats approximately increased by 4-fold relative to that in the hippocampal CA1 regions of the sham group, confirming that Aβ participates in microglial activation. qPCR analysis also revealed that proinflammatory cytokines (IL-1β, IL-6, and TNF-α) levels were elevated whereas the M2 markers (IGF-1, Arg1, and CD206) were reduced in hippocampal tissue homogenates of Aβ-treated rats, suggesting Aβ may stimulate M1-like microglial neuroinflammation (Figure 6c). Accordingly, treatment of rats with Aβ suppressed endogenous ODC and increased AZ protein expression in the hippocampus, implying the ODC/AZ regulatory mechanism may be involved in Aβ-induced microglia M1-polarization (Figure 6d). To precisely determine the expression levels of ODC in Iba1$^+$ cells, we subjected rat hippocampal slices to immunofluorescence staining. The double staining of

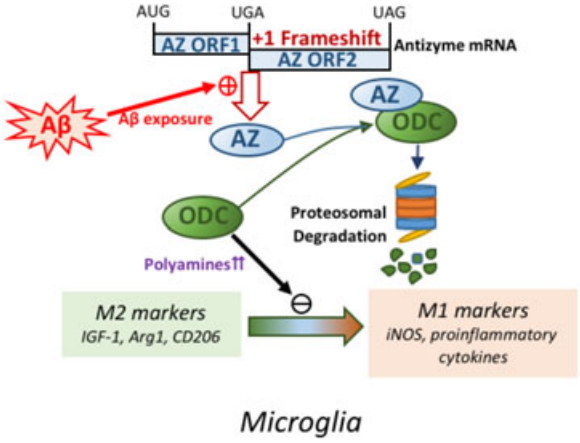

FIGURE 7 A proposed scheme for the potential mechanism of ODC/AZ/polyamine axis in regulation M1 microglial markers activation. Exogenous Aβ can induce AZ mRNA + 1 frameshifting and result in significant upregulation of AZ protein levels. Therefore, intracellular polyamine levels will be suppressed by induction of AZ-mediated ODC proteosomal degradation. The decreased ODC/polyamines may induce M1 microglial markers activation and related proinflammatory responses that finally leads to irreversible neurodegeneration. AZ: antizyme; mRNA: messenger RNA; ODC: ornithine decarboxylase [Color figure can be viewed at wileyonlinelibrary.com]

Iba1 (green) and ODC (red) antibodies showed that most Iba1$^+$ cells (yellow arrows) exhibited significantly decreased ODC protein expression, suggesting that Aβ may reduce ODC expression in activated microglia (Figure 6e).

4 | DISCUSSION

Inflammatory processes are involved in AD progression, and microglia may contribute to Aβ-induced neurotoxicity by releasing various neurotoxic factors (Wang, Tan, Yu, & Tan, 2015). Therefore, an improved understanding of the distinctive phenotypes and regulatory mechanisms of microglia may facilitate the development of strategies that can mitigate AD progression. Dependent on different environmental conditions, activated microglia may exhibit opposing outcomes such as differentiating into proinflammatory M1 or anti-inflammatory M2 microglia. Microglial phenotypes can transition between M1 and M2, indicating that some critical factors can shift microglial polarization from one phenotype to another. Our findings indicated that exogenous Aβ induces the activation of microglial polarization and upregulates the expression of proinflammatory pathways by driving microglia to an activated M1 phenotype. More important, Aβ-induced M1 polarization is likely to reflect decreased levels of ODC and polyamine levels, which may result from an accelerated degradation of ODC and induce AZ synthesis (Figure 7). Interestingly, ODC overexpression can reverse Aβ-induced polyamine reduction and M1 expression, suggesting that the upregulation of the Arg1/ODC/polyamine metabolic pathway may attenuate the Aβ-induced M1 markers expression of BV2 microglia. Increasing evidence suggests that metabolic reprogramming participates in the regulation of microglial M1/M2 polarization (Orihuela et al., 2016). In particular, arginine can be metabolized by the two competing catabolic enzymes arginase or NOS into M1 and M2 microglia, respectively. According to Le Châtelier's principle, once ODC is overexpressed, the arginase pathway will limit arginine availability for the NOS pathway, and ODC itself can further feed into the downstream biosynthesis of polyamines in microglia. Based on these observations, we speculated the regulation of the Arg1/ODC/polyamine axis may be involved in the functional microglia M1/M2 dichotomy.

However, some in vivo studies have also shown that the inhibition of ODC expression by the irreversible inhibitor difluoromethylornithine (DMFO) exerts potential protective effects on AD animal models. For example, Gomes et al. have reported that in mice injected with $A\beta_{25-35}$, the administration of DMFO can counteract Aβ-induced cognitive deficit by inhibiting the polyamine system (Gomes et al., 2014). Similarly, Kan et al. demonstrated that DFMO-treated AD transgenic mice display few CD11b$^+$ cells in the hippocampus, suggesting that ODC inhibition may prevent inflammation-associated AD pathology (Kan et al., 2015). These observations seem inconsistent with our assumption that increased ODC levels may help prevent M1 microglial activation and related proinflammatory responses induced by Aβ. In this regard, previous studies had already demonstrated that DFMO treatment can reduce the number of microglia in the inflammatory brain, suggesting that DFMO has potential applications in the suppression of microglial activation (Nakagawa et al., 1996; Rosi et al., 2012). However, these reports did not assess whether DMFO affects the M1/M2 markers of microglia. ODC and polyamines are essential for the proliferation and repair of various cell types (Hussain et al., 2017). Although excessive polyamine levels can cause inflammatory responses by increasing oxidative stress (Ilmarinen, Moilanen, Erjefält, & Kankaanranta, 2015), the significant depletion of intracellular polyamine levels can also cause the antiproliferative action of human cells (Grossi et al., 2016). In fact, our unpublished data also suggested that the use of DFMO significantly decreases the cell viability of microglia and inhibits the production of cytokines. These results suggest the possibility that DMFO-induced antiAβ neuroprotective effects may be driven by the inhibition of microglial proliferation. In particular, a recent study has shown that in macrophages, ODC deletion markedly enhances M1 response under stress conditions (Hardbower et al., 2017). Microglia are hardly distinguishable from peripheral macrophages (Lai & McLaurin, 2012), thus supporting the concept that ODC may serve as a potent mediator of microglial M1/M2 polarization. However, further studies are needed to determine the precise mechanisms that underlie the Arg1/ODC/polyamine-involved microglial activation of Aβ-induced neuroinflammation in the AD brain.

The regulation of the ODC/AZ/polyamine axis in epithelial cells has been well studied; however, little is known about its roles in microglial polarization. The abundance of ODC in the central nervous system indicates its potential importance in regulating innate immune response (Soulet & Rivest, 2003). As chronic microglial-mediated neuroinflammation is an important feature that contributes

to the pathogenesis of AD, a better understanding of the role of arginine metabolism in the balance of M1/M2 state may help clarify how Aβ induces inflammatory neurodegeneration. Our study revealed the potential mechanism by which ODC and polyamines regulate M1 microglial activation via alterations in AZ + 1 ribosomal frameshifting during Aβ treatment. We further demonstrated that the restoration of ODC protein expression levels in BV2 microglia has profound effects on M1 phenotype inhibition and attenuates Aβ-induced microglial-mediated cytotoxicity. To the best of our knowledge, the current study is the first to consider the involvement of the ODC/polyamine system in the functional M1/M2 dichotomy of microglia in the presence of Aβ toxicity. We improved the current understanding of the link between microglial inflammation and Aβ neurotoxicity at the transition from the iNOS/NO axis to the Arg1/ODC/polyamine axis. We hope that our present findings will support any future efforts to develop therapeutic approaches based on these dynamic cells.

ACKNOWLEDGMENTS

This study was supported by grants from the Ministry of Science and Technology of Taiwan (MOST 106-2320-B-040-021-MY3), and from the National Chung Hsing University and Chung Shan Medical University (NCHU-CSMU-10503).

CONFLICTS OF INTEREST

Authors declare that there are no conflicts of interest.

ORCID

Chih-Li Lin http://orcid.org/0000-0003-4553-3727

REFERENCES

Andreasson, K. I., Bachstetter, A. D., Colonna, M., Ginhoux, F., Holmes, C., Lamb, B., … Van Eldik, L. J. (2016). Targeting innate immunity for neurodegenerative disorders of the central nervous system. *Journal of Neurochemistry*, *138*(5), 653–693.

Bhatia, H. S., Baron, J., Hagl, S., Eckert, G. P., & Fiebich, B. L. (2016). Rice bran derivatives alleviate microglia activation: Possible involvement of MAPK pathway. *Journal of Neuroinflammation*, *13*(1), 148.

Cheng-Chung Wei, J., Huang, H. C., Chen, W. J., Huang, C. N., Peng, C. H., & Lin, C. L. (2016). Epigallocatechin gallate attenuates amyloid beta-induced inflammation and neurotoxicity in EOC 13.31 microglia. *European Journal of Pharmacology*, *770*, 16–24.

Cherry, J. D., Olschowka, J. A., & O'banion, M. (2014). Neuroinflammation and M2 microglia: The good, the bad, and the inflamed. *Journal of Neuroinflammation*, *11*, 98.

Cherry, J. D., Olschowka, J. A., & O'banion, M. K. (2015). Arginase 1 + microglia reduce Abeta plaque deposition during IL-1beta-dependent neuroinflammation. *Journal of Neuroinflammation*, *12*, 203.

Choi, Y., & Park, H. (2012). Anti-inflammatory effects of spermidine in lipopolysaccharide-stimulated BV2 microglial cells. *Journal of Biomedical Science*, *19*, 31.

Clarke, R. M., O'Connell, F., Lyons, A., & Lynch, M. A. (2007). The HMG-CoA reductase inhibitor, atorvastatin, attenuates the effects of acute administration of amyloid-beta1-42 in the rat hippocampus in vivo. *Neuropharmacology*, *52*(1), 136–145.

Colton, C. A. (2009). Heterogeneity of microglial activation in the innate immune response in the brain. *Journal of Neuroimmune Pharmacology*, *4*(4), 399–418.

Dang, Y., Xu, Y., Wu, W., Li, W., Sun, Y., Yang, J., … Zhang, C. (2014). Tetrandrine suppresses lipopolysaccharide-induced microglial activation by inhibiting NF-kappaB and ERK signaling pathways in BV2 cells. *PLoS One*, *9*(8), e102522.

Doens, D., & Fernández, P. L. (2014). Microglia receptors and their implications in the response to amyloid beta for Alzheimer's disease pathogenesis. *Journal of Neuroinflammation*, *11*, 48.

Donat, C. K., Scott, G., Gentleman, S. M., & Sastre, M. (2017). Microglial activation in traumatic brain injury. *Frontiers in Aging Neuroscience*, *9*, 208.

Gad, E. S., Zaitone, S. A., & Moustafa, Y. M. (2016). Pioglitazone and exenatide enhance cognition and downregulate hippocampal beta amyloid oligomer and microglia expression in insulin-resistant rats. *Canadian Journal of Physiology and Pharmacology*, *94*(8), 819–828.

Gomes, G. M., Dalmolin, G. D., Bär, J., Karpova, A., Mello, C. F., Kreutz, M. R., & Rubin, M. A. (2014). Inhibition of the polyamine system counteracts beta-amyloid peptide-induced memory impairment in mice: Involvement of extrasynaptic NMDA receptors. *PLoS One*, *9*(6), e99184.

Grossi, M., Phanstiel, O., Rippe, C., Swärd, K., Alajbegovic, A., Albinsson, S., … Nilsson, B. O. (2016). Inhibition of polyamine uptake potentiates the anti-proliferative effect of polyamine synthesis inhibition and preserves the contractile phenotype of vascular smooth muscle cells. *Journal of Cellular Physiology*, *231*(6), 1334–1342.

Hardbower, D. M., Asim, M., Luis, P. B., Singh, K., Barry, D. P., Yang, C., … Wilson, K. T. (2017). Ornithine decarboxylase regulates M1 macrophage activation and mucosal inflammation via histone modifications. *Proceedings of the National Academy of Sciences of the United States of America*, *114*(5), E751–e760.

Henn, A., Lund, S., Hedtjarn, M., Schrattenholz, A., Porzgen, P., & Leist, M. (2009). The suitability of BV2 cells as alternative model system for primary microglia cultures or for animal experiments examining brain inflammation. *ALTEX: Alternativen zu Tierexperimenten*, *26*(2), 83–94.

Hsieh, M. H., Meng, W. Y., Liao, W. C., Weng, J. C., Li, H. H., Su, H. L., … Ho, Y. J. (2017). Ceftriaxone reverses deficits of behavior and neurogenesis in an MPTP-induced rat model of Parkinson's disease dementia. *Brain Research Bulletin*, *132*, 129–138.

Huang, C. C., Hsu, P. C., Hung, Y. C., Liao, Y. F., Liu, C. C., Hour, C. T., … Liu, G. Y. (2005). Ornithine decarboxylase prevents methotrexate-induced apoptosis by reducing intracellular reactive oxygen species production. *Apoptosis: An International Journal on Programmed Cell Death*, *10*(4), 895–907.

Hussain, T., Tan, B., Ren, W., Rahu, N., Dad, R., Kalhoro, D. H., & Yin, Y. (2017). Polyamines: Therapeutic perspectives in oxidative stress and inflammatory diseases. *Amino Acids*, *49*, 1457–1468.

Ilmarinen, P., Moilanen, E., Erjefält, J. S., & Kankaanranta, H. (2015). The polyamine spermine promotes survival and activation of human eosinophils. *The Journal of Allergy and Clinical Immunology*, *136*(2), 482–484. e411

Kahana, C. (2016). Protein degradation, the main hub in the regulation of cellular polyamines. *The Biochemical Journal*, *473*(24), 4551–4558.

Kan, M. J., Lee, J. E., Wilson, J. G., Everhart, A. L., Brown, C. M., Hoofnagle, A. N., … Colton, C. A. (2015). Arginine deprivation and immune suppression in a mouse model of Alzheimer's disease. *The Journal of Neuroscience*, *35*(15), 5969–5982.

Lai, A. Y., & McLaurin, J. (2012). Clearance of amyloid-beta peptides by microglia and macrophages: The issue of what, when and where. *Future neurology*, *7*(2), 165–176.

Li, H. H., Lin, S. L., Huang, C. N., Lu, F. J., Chiu, P. Y., Huang, W. N., … Lin, C. L. (2016). miR-302 attenuates amyloid-beta-induced neurotoxicity through activation of Akt signaling. *Journal of Alzheimer's disease: JAD*, *50*(4), 1083–1098.

Lin, C. L., Cheng, Y. S., Li, H. H., Chiu, P. Y., Chang, Y. T., Ho, Y. J., & Lai, T. J. (2016). Amyloid-beta suppresses AMP-activated protein kinase

(AMPK) signaling and contributes to alpha-synuclein-induced cytotoxicity. *Experimental Neurology*, *275*(Pt 1), 84–98.

Liu, N., Zhuang, Y., Zhou, Z., Zhao, J., Chen, Q., & Zheng, J. (2017). NF-kappaB dependent up-regulation of TRPC6 by Abeta in BV-2 microglia cells increases COX-2 expression and contributes to hippocampus neuron damage. *Neuroscience Letters*, *651*, 1–8.

McGeer, P. L., & McGeer, E. G. (2015). Targeting microglia for the treatment of Alzheimer's disease. *Expert Opinion on Therapeutic Targets*, *19*(4), 497–506.

McPherson, C. A., Merrick, B. A., & Harry, G. J. (2014). In vivo molecular markers for pro-inflammatory cytokine M1 stage and resident microglia in trimethyltin-induced hippocampal injury. *Neurotoxicity Research*, *25*(1), 45–56.

Murphy, K. J., Miller, A. M., Thelma, R., Cowley, F., Fionnuala cox, F., & Lynch, M. A. (2011). The age- and amyloid-beta-related increases in Nogo B contribute to microglial activation. *Neurochemistry International*, *58*(2), 161–168.

Nakagawa, M., Bellinzona, M., Seilhan, T. M., Gobbel, G. T., Lamborn, K. R., & Fike, J. R. (1996). Microglial responses after focal radiation-induced injury are affected by alpha-difluoromethylornithine. *International Journal of Radiation Oncology, Biology, Physics*, *36*(1), 113–123.

Orihuela, R., McPherson, C. A., & Harry, G. J. (2016). Microglial M1/M2 polarization and metabolic states. *British Journal of Pharmacology*, *173*(4), 649–665.

Peña-Altamira, E., Petralla, S., Massenzio, F., Virgili, M., Bolognesi, M. L., & Monti, B. (2017). Nutritional and pharmacological strategies to regulate microglial polarization in cognitive aging and Alzheimer's disease. *Frontiers in Aging Neuroscience*, *9*, 175.

Ramani, D., De Bandt, J. P., & Cynober, L. (2014). Aliphatic polyamines in physiology and diseases. *Clinical Nutrition (Edinburgh, Scotland)*, *33*(1), 14–22.

Rosi, S., Ferguson, R., Fishman, K., Allen, A., Raber, J., & Fike, J. R. (2012). The polyamine inhibitor alpha-difluoromethylornithine modulates hippocampus-dependent function after single and combined injuries. *PLoS One*, *7*(1), e31094.

Roy, A., Jana, A., Yatish, K., Freidt, M. B., Fung, Y. K., Martinson, J. A., & Pahan, K. (2008). Reactive oxygen species up-regulate CD11b in microglia via nitric oxide: Implications for neurodegenerative diseases. *Free Radical Biology & Medicine*, *45*(5), 686–699.

Soulet, D., & Rivest, S. (2003). Polyamines play a critical role in the control of the innate immune response in the mouse central nervous system. *The Journal of Cell Biology*, *162*(2), 257–268.

Tang, Y., & Le, W. (2016). Differential roles of M1 and M2 microglia in neurodegenerative diseases. *Molecular Neurobiology*, *53*(2), 1181–1194.

Wang, W. Y., Tan, M. S., Yu, J. T., & Tan, L. (2015). Role of pro-inflammatory cytokines released from microglia in Alzheimer's disease. *Annals of Translational Medicine*, *3*(10), 136.

SUPPORTING INFORMATION

Additional supporting information may be found online in the Supporting Information section at the end of the article.

How to cite this article: Cheng Y-W, Chang C-C, Chang, T-S, et al. Aβ stimulates microglial activation through antizyme-dependent downregulation of ornithine decarboxylase. *J Cell Physiol*. 2019;234:9733–9745. https://doi.org/10.1002/jcp.27659